Dynamic determination of the dendritic growth direction within a complex-phase-field model

Royce Kam and Herbert Levine
Department of Physics, and Institute for Nonlinear Science, University of California, San Diego, La Jolla, California 92093-0402
(Received 17 May 1995)

We generalize the standard phase-field model of solidification to accommodate a complex-valued order parameter. This model allows for a direct incorporation of crystalline anisotropy and also allows for a nontrivial dynamical competition between bulk "bending" energies of the axes as compared to anisotropic surface energies. We illustrate this by studying a specific case of competing anisotropies; simulations demonstrate the nontrivial spatio-temporal evolution of the dendritic growth direction.

PACS number(s): 68.70.+w

Since their advent, phase-field models have become an important tool in the study of interfacial patterns in diffusion-limited growth [1–3]. In particular, they have been used to move beyond the study of isolated growth elements such as single dendrites toward investigation of the overall global morphology of the evolving pattern [4]. The standard phase-field approach assumes that the solid can be described by a real order parameter field; the time evolution of this field is coupled to a diffusing variable to form a complete microscopic model of the solidification process. This work suggests a useful generalization of this method in which the solid is described instead by a complex field.

Part of the motivation for this work lies in trying to understand the patterns that can occur in the diffusion-limited growth of condensed-phase monolayers [5–7]. Here, the interesting phenomena range from equilibrium interfaces which exhibit sharp cusps [8,9], to the standard nonequilibrium patterns involving fractals or stable dendrites, to the enigmatic "spiral" dendrite [10] seen in nonreflection symmetric molecules. In these cases, there seems to be the interesting possibility that the various order parameters of the condensed phase vary with position in the bulk, possibly forming defects and/or domain walls, and that these interact with the condensed-expanded interface. While we have nothing specific to say about these patterns in this Brief Report, extensions of our current technology to allow for the correct incorporation of crystalline anisotropy as a consequence of rotational symmetry breaking in the condensed phase is a prerequisite for making a microscopic model relevant for future efforts on monolayer systems.

The standard phase-field model describing diffusion-limited solidification is defined by the equations

$$-\Gamma\frac{d\Psi}{dt} = \frac{\delta F[\Psi,U]}{\delta\Psi}, \tag{1}$$

$$D\nabla^2 U - \frac{dU}{dt} = -\frac{1}{2}\frac{d\Psi}{dt}, \tag{2}$$

where Ψ is a real-valued order parameter describing the phase of the material and U is a dimensionless temperature field, measuring the deviation from the melting temperature T_m (in units of L/C_p, the ratio of the latent heat to the heat capacity of the material). Γ is the characteristic relaxation time for the order parameter dynamics, and D is the heat diffusivity of the material. $F[\Psi,U]$ is the free energy functional [11]

$$F[\Psi,U] = \int d\vec{r}\alpha(\nabla\Psi)^2 + \beta(\Psi^2-1)^2 + cU\Psi. \tag{3}$$

The first term measures the energy cost for spatial inhomogeneity of the order parameter. The second term is a typical "double well," with the minimum at $\Psi=+1$ representing the solid phase, and the minimum at $\Psi=-1$ representing the liquid phase. At the equilibrium temperature ($U=0$), the two minima have the same height (energy) so that neither phase is favored. Away from equilibrium, the third term couples the phase to the temperature by tilting the wells to favor the appropriate phase. The right-hand side of (2) represents the latent heat released at the interface as the liquid solidifies [1]. Note that this is the simplest phase-field model describing diffusion-limited solidification. Models with greater thermodynamic consistency have been formulated by Penrose and Fife [12].

One basic problem with the above formulation is that it treats the crystalline solid as isotropic. Not only is this quantitatively untrue, but in fact it has been shown that anisotropy is perhaps the most crucial determinant of pattern morphology in diffusion-limited growth. Previous workers have remedied this problem by introducing anistropy with respect to some *a priori* fixed set of axes. In one method, higher derivatives are added to the free energy [4]. Another method is to expand the Hamiltonian in a (discrete) Fourier series which, in the continuum limit, results in higher order derivatives of the (real) order parameter in the dynamic equations [2]. Both methods eliminate the possibility of there being interesting dynamics in the local orientational order parameter and are therefore ill-suited to systems where such dynamics might be important. We therefore wish to directly incorporate the orientational order into the phase of a complex order parameter.

Our complex order parameter can be written as

$$\Psi = |\Psi|e^{in\theta}, \tag{4}$$

where n is the order of the rotational symmetry of the material and θ is the angle the crystal planes of the solid make with respect to some reference axis. The magnitude of the new order parameter plays the role of the old, real-valued order parameter; it indicates whether the material is in solid or liquid phase. The phase denotes the orientational order in a familiar manner; under (passive) rotation by angle α, $\Psi \to \Psi e^{-in\alpha}$. The previous Landau-Ginzburg equation (1) is replaced by

$$-\Gamma \frac{d\Psi}{dt} = \frac{\delta F[\Psi, U]}{\delta \Psi^*}. \tag{5}$$

In addition, we replace (2) with

$$D\nabla^2 U - \frac{dU}{dt} = -\frac{d|\Psi|^2}{dt}. \tag{6}$$

This reflects the fact that the release of latent heat depends only on the change from liquid to solid; this information is contained in the magnitude and not in the phase of the order parameter.

We now turn our attention to the details of the free energy functional. We choose a new "double-well" potential

$$F_0[\Psi, U] = \int d\vec{r}\, \kappa|\nabla\Psi|^2 + \alpha[|\Psi|^2 - 2|\Psi|^4 + |\Psi|^6 + T|\Psi|^2 \tanh(\lambda U)], \tag{7}$$

which contains no odd powers of $|\Psi|$. Clearly, F_0 is invariant under rotations of the coordinate axes. The double well has two equal minima at $|\Psi|$=0 (liquid) and $|\Psi|$=1 (solid). Note that this form of the potential is similar to that used by Kupferman and Shochet in their simulations [4].

The key to understanding how this approach can be used to get physical anisotropy is to consider a term of the form

$$F_n[\Psi] = \frac{1}{2}\int d\vec{r}|\Psi|^2 \partial_z^n \Psi, \tag{8}$$

where $z = x + iy$. It is invariant under coordinate rotations since a rotation of the axes counterclockwise by an angle α causes $\partial_z^n \to e^{in\alpha}\partial_z^n$, whereas we have assumed that $\Psi \to \Psi e^{-in\alpha}$. We add $F_n + F_n^*$ to the free energy F_0, and consider the extra contribution to the surface tension induced by this term. The surface tension is just the additional free energy per unit area introduced by requiring the presence of a boundary between two phases in equilibrium ($U = 0$). Integration by parts of the term in question yields (for n even)

$$\frac{1}{2}\int d\vec{r}\left(\partial_z^n|\Psi|^2\right)\Psi + \text{c.c.} \tag{9}$$

Since the physical solid-liquid interface is very thin, we know that the largest derivatives of $|\Psi|$ will be in a direction normal to the interface, which can be thought of as locally planar. Suppose this direction makes some angle ϕ with respect to the positive x axis. Then, we can approximately take $|\Psi|$ to be a function only of the coordinate along this direction, $u \equiv (x\cos\phi + y\sin\phi)$. Then $\partial_z|\Psi| = e^{-i\phi}\frac{d|\Psi|}{du}$. Thus, Eq. (9) reduces to

$$\frac{1}{2}\int dS\; e^{in(\theta-\phi)}\int_{+\infty}^{-\infty} du \frac{d^n\left(|\Psi|^2\right)}{du^n}|\Psi| + \text{c.c.}, \tag{10}$$

where the integration decomposes into a surface integral and a line integral in the direction normal to the surface. This latter integral is evaluated using the equilibrium $|\Psi|$ profile for a planar interface (see, for example, Ref. [1]). Thus, the surface tension is simply proportional to $\cos n(\theta - \phi)$. The maxima of this function will determine the directions of dendritic growth.

More generally, a free energy of $(e^{in\theta_0}F_n + \text{c.c.})$ will yield a surface tension proportional to $\cos n(\theta + \theta_0 - \phi)$. Hence, the parameter θ_0 allows us to choose the dendrite direction with respect to the crystal axes. Also, it is easy to see that an n-fold order parameter can be used to construct surface energy terms which are higher harmonics of n. For example, one possible second harmonic term is just

$$F_n^{(2)}[\Psi] = \frac{1}{2}\int d\vec{r}|\Psi|^2\partial_z^{2n}\Psi^2\,. \tag{11}$$

We have performed simulations of the above complex-phase-field model for the case $n = 2$, i.e., using a free energy

$$F[\Psi, U] = F_0 + \eta_2\left(e^{2i\theta_0}F_2 + e^{-2i\theta_2}F_2^*\right) + \eta_4\left(F_2^{(2)} + F_2^{(2)*}\right). \tag{12}$$

We have rescaled the equations so that the length unit is $l_k \equiv D\Gamma/\sqrt{\kappa}$ (the "kinetics-limited diffusion length"), the unit of time is l_k^2/D (the related diffusion time), and ϵ can be interpreted as the interface thickness (details of rescaling in Ref. [13]).

Equations (5) and (6) were solved numerically using an explicit scheme to integrate the equations in time on a triangular lattice. Grid sizes were typically 100×115 grid points. Unless otherwise specified, the results described

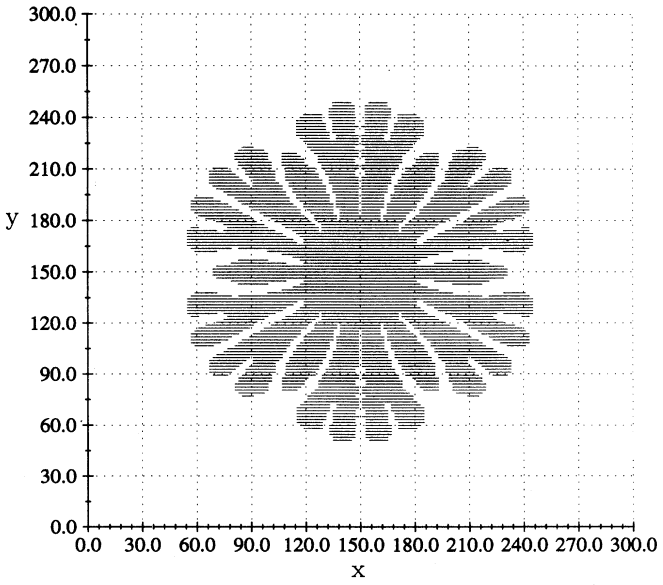

FIG. 1. Sixfold symmetry for branching pattern at $\Delta = 0.65$.

below used $\epsilon = 0.4$, $\lambda = 10$, $\alpha = 1.0$, $T = 0.6$, and $-U(\infty) \equiv \Delta = 0.6$. Initial seeds were circles with radii of 6. In the figures which follow, points for which $|\Psi| \geq 0.5$ (the "solid") are represented by line segments whose orientations indicate the inclination of the crystal planes with respect to the x axis.

Note that the discretization of space in a simulation introduces an artificial "lattice anisotropy" in a model. It has been demonstrated that a grid with extremely fine resolution (e.g., 2500×2500 grid points) can minimize these effects [4]. Unfortunately, we lacked the computing resources to run such large scale simulations and were forced to rely on underresolved simulations. To obtain some idea of the lattice anisotropy implicitly introduced by our grid, we ran an isotropic free energy ($\eta_2 = \eta_4 = 0.0$) at an undercooling $\Delta = 0.65$. Examination of the resulting plot (Fig. 1) shows that the lattice anisotropy is too weak to produce stable dendrites, and instead we see a dense-branching morphology. Note, however, that the sixfold symmetry of the lattice is evident in the overall growth pattern, showing that the directions obtained by $\pi/3$ rotations from $\hat{y}$ are the fastest growing directions.

Next, we tested the ability of the model to exhibit twofold dendrites. We simulated the growth of an initial seed with crystal axes parallel to the x axis and dendritic growth perpendicular to the crystal axes [Fig. 2(a)] with the parameters $\eta_2 = 0.32$, $\eta_4 = 0.0$, $\theta_0 = 0.0$. The same parameters run on an initial seed with crystal axes rotated $\frac{\pi}{3}$ counterclockwise from the x axis [Fig. 2(b)] indicate how the dendrite directions are determined by the orientation of the crystal axes. In addition, identical

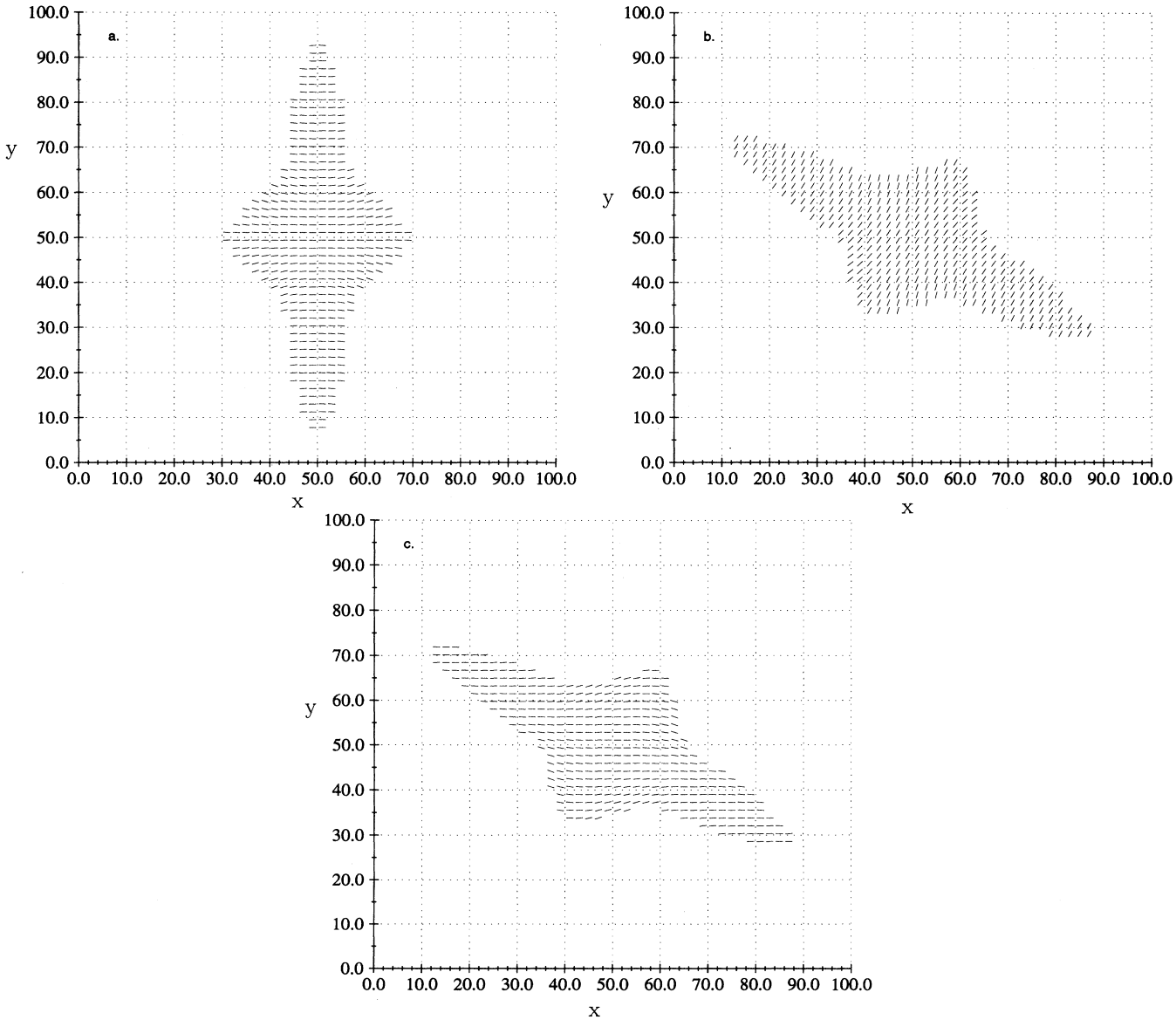

FIG. 2. (a) Twofold dendrites for $\Delta = 0.60$, $\eta_2 = 0.32$, $\eta_4 = \theta_2 = 0.0$, and crystal planes of initial seed parallel to the x axis. (b) Rotation of twofold dendrites obtained by rotating crystal planes of initial seed $\frac{\pi}{3}$ counterclockwise. (c) Rotation by setting $\theta_2 = \frac{\pi}{3}$ with the crystal planes of the initial seed parallel to the x axis.

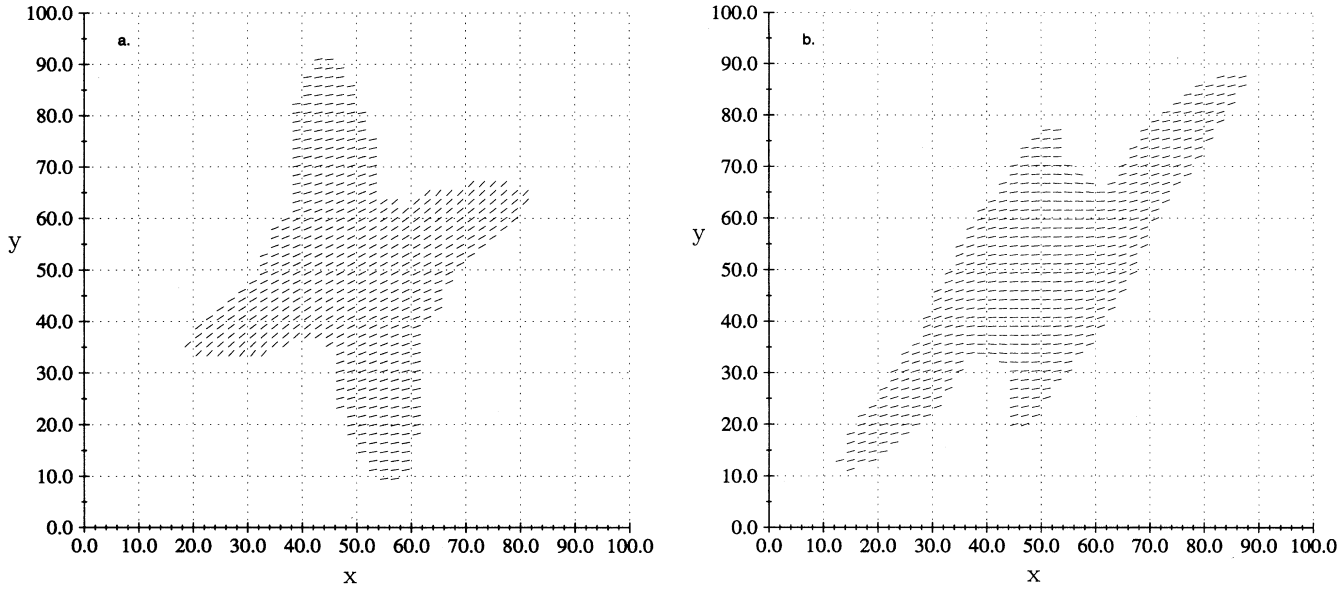

FIG. 3. (a) Competition between explicit fourfold and implicit lattice anisotropy for $\Delta = 0.60$, $\eta_2 = 0.0$, $\eta_4 = 0.24$ with the crystal planes of the initial seed inclined $\frac{\pi}{6}$ from the $+x$ axis. (b) Strongly nonreflection-symmetric dendrite obtained for $\eta_2 = 0.32$ and $\eta_4 = 0.12$.

parameters with $\theta_0 = \frac{\pi}{3}$ and an initial seed with crystal axes parallel to the x axis [Fig. 2(c)] demonstrate how the dendritic growth direction with respect to the crystal axes may be changed. In each case, the growth direction is along a symmetry line of the lattice allowing the dendrite tip to remain symmetric in spite of the lattice anisotropy.

For $\eta_2 = 0.0$ and $\eta_4 > 0$, fourfold dendrites should grow parallel and normal to the crystal axes. We simulated growth with $\eta_4 = 0.24$ and an initial seed rotated counterclockwise by $\frac{\pi}{6}$ with respect to the x axis [Fig. 3(a)]. The dendrites which attempt to grow parallel to the lattice planes are also growing along lattice symmetry directions. These behave normally aside from perhaps a minor asymmetry induced by the nonsymmetric arrangement of the neighboring dendrites. On the other hand, we find dendrites growing in the up and down directions; examination of the vectors shows that the crystal axes have been bent in the bulk so as to accommodate the lattice anisotropy. This dynamical possibility (which of course depends on the size of the crystal, the relative strength of the bending energy as compared to the surface energy, etc.) is completely absent in the standard phase-field approach.

The last case we present resulted from an initial seed with crystal axes parallel to the x axis and the parameters $\eta_2 = 0.32$, $\eta_4 = 0.12$, and $\theta_0 = -\frac{\pi}{3}$ [Fig. 3(b)]; here, the dominant twofold dendrites prefer to grow $\frac{\pi}{3}$ clockwise from the normal to the crystal axes, while the weaker fourfold dendrites prefer to grow along the perpendiculars and the normals to the crystal axes. Examination of the orientation of the lattice planes provides explicit verification of the claim by Brener *et al.* that competition between two nonaligned directions leads to nonreflection symmetric growth along an intermediate angle [14]. This case also demonstrates bending of the crystal planes, up to a maximum of 24°.

In summary, we have introduced a complex phase-field model in which the argument of the complex order parameter encodes the local breaking of rotational symmetry. We have shown that this model provides a framework for allowing the dendritic growth direction to become a dynamic variable within the model itself. We hope that this ability of the model will become a useful tool in tackling patterns in monolayer "crystallization," where there is increasing evidence that the crystal shape arises from a complex interplay between the bulk structure and the interfacial energies.

We would like to acknowledge useful communications with O. Shochet.

[1] J. B. Collins and H. Levine, Phys. Rev. B **31**, 6119 (1985).
[2] G. Caginalp and P. C. Fife, Phys. Rev. B **34**, 4940 (1986).
[3] J. S. Langer, *Models of Pattern Formation in First-Order Phase Transitions* (World Scientific, Singapore, 1986).
[4] R. Kupferman, O. Shochet, and E. Ben-Jacob, Phys. Rev. E **50**, 1005 (1994).
[5] C. M. Knobler, Science **249**, 870 (1990).
[6] W. M. Heckl, M. Losche, D. A. Cadenhead, and H. Mohwald, Eur. Biophys. J. **14**, 11 (1986).
[7] Xiao-Min Yang *et al.*, Phys. Lett. A **193**, 195 (1994).
[8] D.T. Schwartz, M. Tsao, and C. M. Knobler, J. Chem. Phys. **101**, 8258 (1994).
[9] J. Rudnick and R. Bruinsma, Phys. Rev. Lett. **74**, 2491 (1995).
[10] R. Weis and H. McConnell, Nature **310**, 47 (1984).
[11] P. C. Hohenberg and B. I. Halperin, Rev. Mod. Phys. **49**, 435 (1977).
[12] O. Penrose and P. C. Fife, Physica D **69**, 107 (1993).
[13] R. Kupferman, O. Shochet, E. Ben-Jacob, and Z. Schuss, Phys. Rev. B **46**, 16 045 (1992).
[14] E. Brener and H. Levine, Phys. Rev. A **43**, 883 (1991).